Annex U2 – VSDC FINAL REPORT – CHAPTER Y

Note: This Annex appears in its original format.

Final

Chapter Y – COMPARISON OF THE PERFORMANCE OF THE FED-ALPHA VEHICLE PREDICTED BY NWVPM WITH TEST RESULTS (PHASE II)

Vehicle Systems Development Corporation
Toronto, Ontario, Canada

Y.1 GOALS

The objective of this chapter is to highlight the comparison of the performance of the FED-Alpha vehicle predicted by the Nepean Wheeled Vehicle Performance Model (NWVPM), developed by Vehicle Systems Development Corporation (VSDC), and test results obtained by Keweenaw Research Center (KRC), Michigan Technological University. It constitutes the major part of the work performed by VSDC for the Phase II of the Next Generation NATO Reference Mobility Model Cooperative Demonstration of Technology event.

Y.2 INTRODUCTION

This chapter highlights the comparison of the performance of the FED-Alpha vehicle predicted by NWVPM on various types of terrain with that measured by KRC. The approaches to the development of NWVPM and its unique features have been outlined in Chapter X.

In this chapter, the following topics are discussed:

(A) Design parameters of the FED-Alpha vehicle used in NWVPM for predicting its performance.
(B) Measured terrain parameters for the test sites where the FED-Alpha vehicle was tested.
(C) Performance of the FED-Alpha vehicle predicted by NWVPM with measured terrain data for the test sites.
(D) Comparison of the performance of the FED-Alpha vehicle predicted by NWVPM with test data obtained by KRC.
(E) Simulations of the performance of the FED-Alpha vehicle by NWVPM at the design of experiment (DOE) points for uncertainty quantification maps.

Y.3 MAJOR DESIGN PARAMETERS OF THE FED-ALPHA VEHICLE

The major design parameters of the FED-Alpha vehicle used in the prediction of the drawbar performance by NWVPM have been presented in Chapter X, Section X.4. For the convenience of the reader, the major vehicle design parameters of the FED-Alpha vehicle are reproduced in Table Y-1, and the major tire parameters for the vehicle is presented in Table Y-2. A sketch of the side view of the FED-Alpha vehicle, as part of the output of NWVPM, is shown in Figure Y-1.

Table Y-1: Major vehicle parameters of the FED-Alpha vehicle.

Total vehicle weight	53.755 kN
Front axle load (static)	27.845 kN
Rear axle load (static)	25.910 kN
Front axle track width	197.60 cm
Rear axle track width	195.91 cm
Front axle suspension stiffness (average)	2.941 kN/cm
Rear axle suspension stiffness (average)	3.693 kN/cm
CG longitudinal location from the center of front axle	159.16 cm
CG height from the ground	99.14 cm
Drawbar hitch longitudinal location from the center of front axle	423.78 cm
Drawbar hitch height from the ground	108.71 cm
Ground clearance	40.64 cm

Table Y-2: Major tire parameters of the FED-Alpha vehicle.

Tire name	Goodyear 335/65R22.5
Effective tire radius	45.3 cm
Tread width	33.50 cm
Lug area/Carcass area (Specific/Nominal contact area)	0.58
Lug height	1.60 cm
Lug width	6.0 cm
Inflation pressure	241 kPa
Ground pressure (Tire load/Nominal contact area)	247 kPa

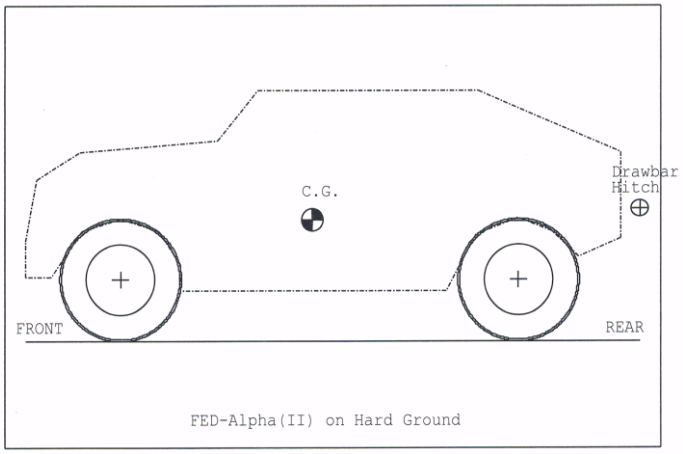

Figure Y-1: A sketch of the side view of the FED-Alpha vehicle, as part of the output from NWVPM.

Y.4 TERRAIN DATA FOR THE TEST SITES FOR PREDICTING THE PEFORMANCE OF THE FED-ALPHA VEHICLE BY NWVPM

Terrain data for the test sites where the performance testing of the FED-Alpha vehicle was conducted were obtained on two separate occasions, one on June 5 and the other on June 29, 2018. The drawbar performance of the vehicle was predicted by NWVPM with these two different sets of terrain data obtained on June 5 and June 29, 2018.

The pressure-sinkage test data obtained by KRC are characterized by the Bekker equation [1, 2, 3]:

$$p = \left(\frac{k_c}{b} + k_\varphi \right) z^n \qquad \text{(Y-1)}$$

where b is the radius of a circular contact area or the width of a rectangular contact area; k_c, k_φ and n are the Bekker pressure-sinkage parameters; p is pressure; z is sinkage.

In the early stage of development of terramechanics, it was thought that k_c and k_φ might be related to the cohesive and frictional properties of the terrain, respectively. As more terrain data, particularly field test data, become available, the current view is that k_c and k_φ are primarily curve fitting parameters and may not have definitive physical meaning.

The Bekker equation (Y-1) indicates that for a smaller plate sinking to the same depth, the pressure required should be higher than that for a larger plate. In the field, owing to a variety of reasons, the measured pressure-sinkage relationship may not exhibit the same trend as that indicated by the Bekker Equation. For instance, test data may show that with a larger plate, the pressure at various depths may be higher than that with a smaller plate. This leads to a negative value for k_c.

To avoid the use of negative values for pressure-sinkage parameters, the following equation may be used [1, 2, 3],

$$p = k_{eq}\, z^n \qquad \text{(Y-2)}$$

where k_{eq} may be interpreted as an equivalent pressure-sinkage parameter.

Equation (Y-2) indicates that pressure p is not related to the radius (or effective radius) or the size of the contact area. It may be considered as a special form of the Bekker equation, where $k_c = 0$, and k_{eq} is equivalent to k_φ.

In this study, if the values of k_c and k_φ are positive, then the original Bekker equation, (i.e., Equation (Y-1)), will be used to characterize the pressure-sinkage relation of the terrain. On the other hand, if the value of either k_c or k_φ is negative, then Equation (Y-2) will be employed to characterize the pressure-sinkage relationship of the terrain.

For a multi-axle wheeled vehicle with the axles having the same track (tread), the succeeding wheels will run in the ruts of the preceding wheels. The terrain under the succeeding wheels will be subject to the effects of repetitive loading. To realistically predict vehicle performance, it is necessary to take into account terrain response to repetitive loading [1, 2]. Terrain

stiffness k_u characterizing the unloading and reloading behaviour can be expressed by the following equation [1, 2],

$$k_u = k_0 + A_u z_u \quad \text{(Y-3)}$$

where k_0 and A_u are repetitive loading parameters of the terrain; z_u is the sinkage where unloading begins.

The pressure-sinkage relationship during unloading or reloading can be expressed by

$$p = p_u - k_u (z_u - z) \quad \text{(Y-4)}$$

where p and z are the pressure and sinkage during unloading or reloading; p_u is the pressure where unloading begins.

In this study, to characterize the shear stress-shear displacement relationship of terrain, the Janosi-Hanamoto equation is used [4],

$$s = (c + p \tan\varphi)(1 - \exp(-j / K) \quad \text{(Y-5)}$$

where c is cohesion; j is shear displacement; K is the shear deformation parameter; p is the normal pressure on the shear surface; s is shear stress; φ is the angle of friction of the terrain (or the angle of internal shearing resistance of the terrain).

For rubber-terrain shearing characteristics, an equation similar to Equation (Y-5) may be used, where adhesion c_a, angle of rubber-terrain friction φ_r, and rubber-terrain shear deformation parameter K_r replace c, φ, and K in Equation (Y-5), respectively.

Y.4.1 Terrain data collected by KRC on June 5, 2018

The mean values of terrain parameters for the fine-grained soil-dry (FGS-Dry) were obtained from two test sets (Test Sets 9 and 10), for fine-grained soil-wet (FGS-Wet) from two test sets (Test Sets 17 and 18), and for coarse-grained soil-dry (CGS-Dry) from three test sets (Test Sets 12, 13, and 14) on June 5, 2018. The mean values of terrain parameters for 2NS Sand were obtained from two test sets (Test Sets 1 and 2) on June 1, 2018.

Table Y-3 shows the mean values of the pressure-sinkage parameters, n, k_c, and k_φ (or k_{eq}), and the repetitive loading parameters, k_0 and A_u, for the four types of terrain.

Table Y-3: Mean values of the pressure-sinkage and repetitive loading parameters measured by KRC.

Terrain type	n	k_c, kN/m^{n+1}	k_φ, kN/m^{n+2}	k_{eq}, kN/m^{n+2}	k_0, kN/m^3	A_u, kN/m^4
FGS-Dry	1.74	-	-	318,070	93,970	3,746,425
FGS-Wet	3.3	3,216	126,639	-	0	1,334,085
CGS-Dry	0.6	55	1,099	-	120,421	2,309,750
2NS Sand	0.5	52	441	-	90,523	1,317,628

Table Y-4 shows the mean values of the internal shear parameters of the terrain: cohesion c, angle of friction φ, and shear deformation parameter K, and the rubber-terrain shear parameters: adhesion c_a, angle of friction φ_r, and shear deformation parameter K_r for the four types of terrain.

Table Y-4: Mean values of the terrain internal and rubber-terrain shear parameters measured by KRC.

Terrain type	c, kPa	$\varphi°$	K, cm	c_a, kPa	$\varphi_r°$	K_r, cm
FGS-Dry	1.38	36.7	1.78	0	28.8	0.76
FGS-Wet	3.45	35.2	3.05	0.69	28.8	0.76
CGS-Dry	1.38	31.4	2.03	0	26.7	1.02
2NS Sand	1.38	32	2.03	0	26.7	0.76

Y.4.2 Terrain data collected by KRC on June 29, 2018

The values of terrain parmeters for FGS-Dry are obtained from one test set (Test Set 34), for FGS-Wet from one test set (Test Set 36), and for CGS-Dry again from one test set (Test Set 35) on June 29, 2018.

Table Y-5 shows the values of the pressure-sinkage parameters, n, k_c, and k_φ (or k_{eq}) obtained on June 29, 2018. The test data for repetitive loading parameters, k_0 and A_u of the three types of terrain for June 29, 2018 were not provided by KRC, and the values of k_0 and A_u shown in Table Y-3 were used in vehicle performance predictions by NWVPM.

Table Y-5: The pressure-sinkage and repetitive loading data for June 29, 2018.

Terrain type	n	k_c, kN/m^{n+1}	k_φ, kN/m^{n+2}	k_{eq}, kN/m^{n+2}	k_0, kN/m^3	A_u, kN/m^4
FGS-Dry	1.42	5,085	6,259		93,970	3,746,425
FGS-Wet	4.62	-	-	65,749,075	0	1,334,085
CGS-Dry	1.09	-	-	3,919	120,421	2,309,750

Table Y-6 shows the mean values of the internal shear parameters: cohesion c, angle of friction φ, and shear deformation parameter K, and the rubber-terrain shear parameters: adhesion c_a, angle of friction φ_r, and shear deformation parameter K_r for the three types of terrain obtained on June 29, 2018.

Table Y-6: Mean values of the terrain internal and rubber-terrain shear parameters measured by KRC, dated June 29, 2018.

Terrain type	c, kPa	$\varphi°$	K, cm	c_a, kPa	$\varphi_r°$	K_r, cm
FGS-Dry	1.58	34.1	2.22	0	27.6	0.51
FGS-Wet	2.37	37.74	2.08	0.46	28.3	0.96
CGS-Dry	0.99	31.5	2.45	0	27.5	1.01

The pressure-sinkage characteristics of the three types of terrain measured on June 29, 2018 are shown in Figure Y-2, based on the pressure-sinkage parameters given in Table Y-5. It indicates that FGS-Dry is the firmest among the three types of terrains examined. For FGS-Wet, the pressure increases slowly with the increase of sinkage at the initial stage and then increases rapidly with the further increase of sinkage. It exhibits the characteristics of a terrain with soft layer at the top and hard layer at the bottom.

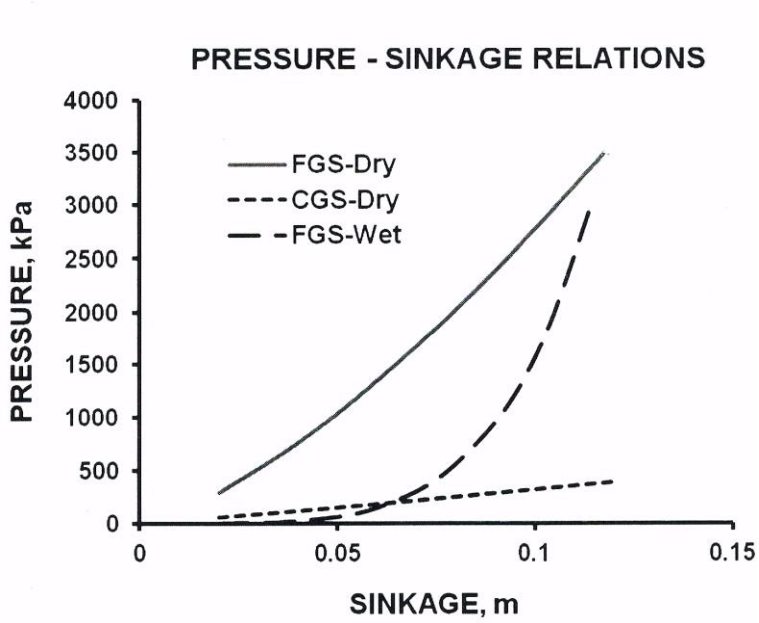

Figure Y-2: Pressure-sinkage characteristics of FGS-Dry, FGS-Wet and CGS-Dry.

Y.5 COMPARISON OF THE MEASURED AND PREDICTED PERFORMANCE BY NWVPM OF THE FED-ALPHA VEHICLE ON VARIOUS TYPES OF TERRAIN

Steady-state drawbar performance is a cornerstone for evaluating or comparing off-road vehicle mobility. Consequently, the common practice is to measure the drawbar pull coefficient-slip relationship under steady-state conditions. The drawbar pull coefficient is the ratio of drawbar pull to vehicle weight. The drawbar performance testing on June 5, 2018 was conducted, however, under dynamic (time-varying or transient) conditions. Additional drawbar performance testing under steady-state conditions was subsequently performed on June 29, 2019. In the following, the FED-Alpha vehicle performance, measured under dynamic and steady-state conditions on June 5 and June 29, 2018, respectively, was compared with the predicted performance obtained by NWVPM, with the corresponding terrain data.

Y.5.1 Comparison of the measured vehicle performance under dynamics conditions on June 5, 2018 with that predicted by NWVPM

Y.5.1.1 Vehicle drawbar performance measured under dynamic conditions on June 5, 2018

As noted previously, on June 5, 2018 vehicle performance testing was conducted under dynamic (time-varying or transient) conditions. As an example, Figure Y-3 shows the variation of the measured drawbar pull with time for one of the tests performed on that date. It can be seen that during the test, the drawbar pull varied in a wide range over the period from 6 s to 24 s, and was far from steady-state conditions. Figure Y-4 shows the variation of vehicle speed with time, corresponding to that shown in Figure Y-3. It is noted that during the test, vehicle speed varied greatly with time. During the first half of the test from 6 s to 12 s the vehicle was mostly accelerating, while from 12 s to 21 s the vehicle was primarily decelerating.

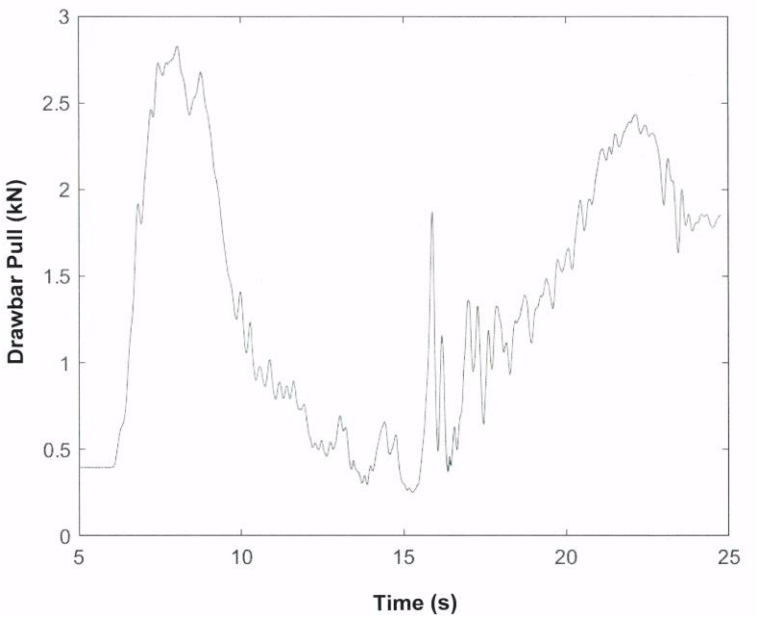

Figure Y-3: Variation of drawbar pull with time during a test on June 5, 2018.

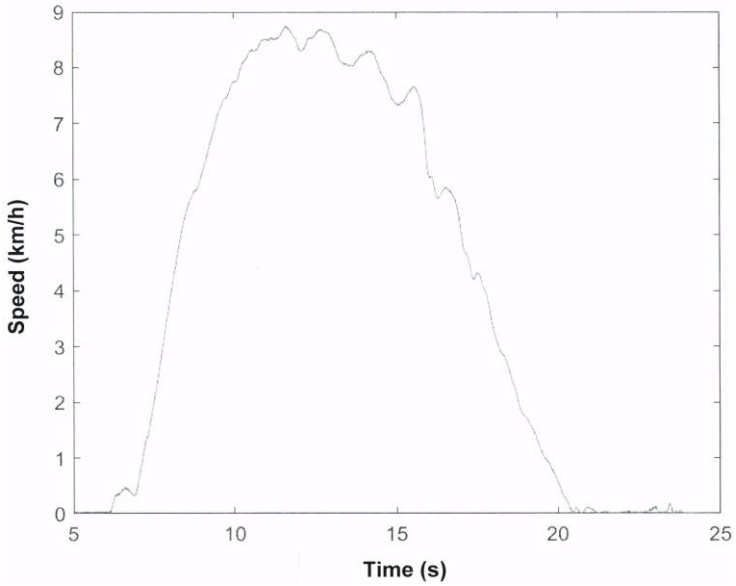

Figure Y-4: Variation of vehicle speed with time during a test on June 5, 2018.

To take into account the effect of acceleration/deceleration on the drawbar pull and to obtain the corresponding steady-state drawbar pull coefficient-slip relationship, corrections were made to the originally measured data. The drawbar pull coefficient–slip curves, corrected for the inertial effect of vehicle mass, on the three types of terrain, fine-grained soil-dry (FGS-Dry), fine-grained soil-wet (FGS-Wet), and coarse-grained soil-dry (CGS-Dry), are shown in Figure Y-5, Y-6, and Y-7, respectively.

It should be pointed out that while the values of the measured drawbar pull coefficient shown in the figures have been corrected for the inertial effect of vehicle mass, it is uncertain that all other possible dynamic effects on vehicle-terrain interaction have been properly account for in the corrected drawbar pull coefficient-slip relationships shown in Figures Y-5, Y-6, and Y-7. These would include the effect on performance of varying shear rate at the tire-terrain interface caused by the variation of vehicle speed, and of the fluctuation of the dynamic normal load on the tire caused by the variation of drawbar pull.

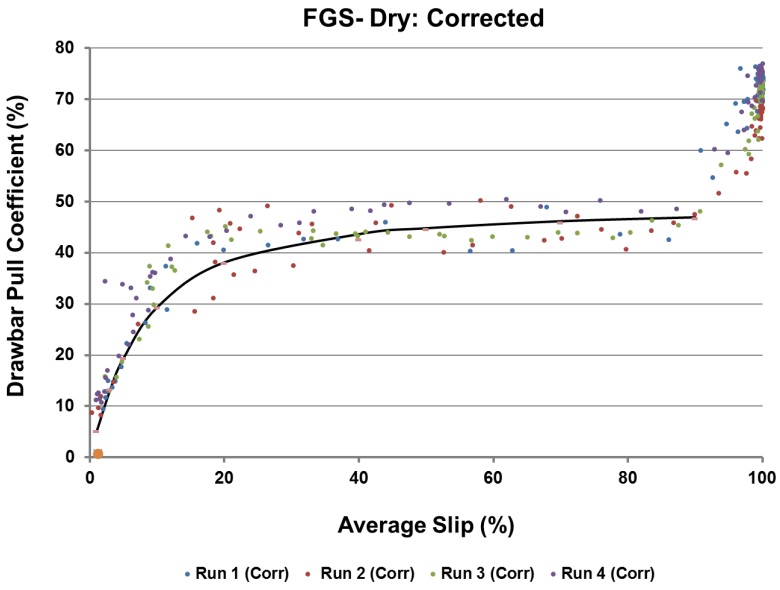

Figure Y-5: Comparison of the drawbar pull coefficient-slip relationship predicted by NWVPM (solid line) with that measured (with corrections for the inertial effect of vehicle mass) on fine-grained soil-dry of June 5, 2018.

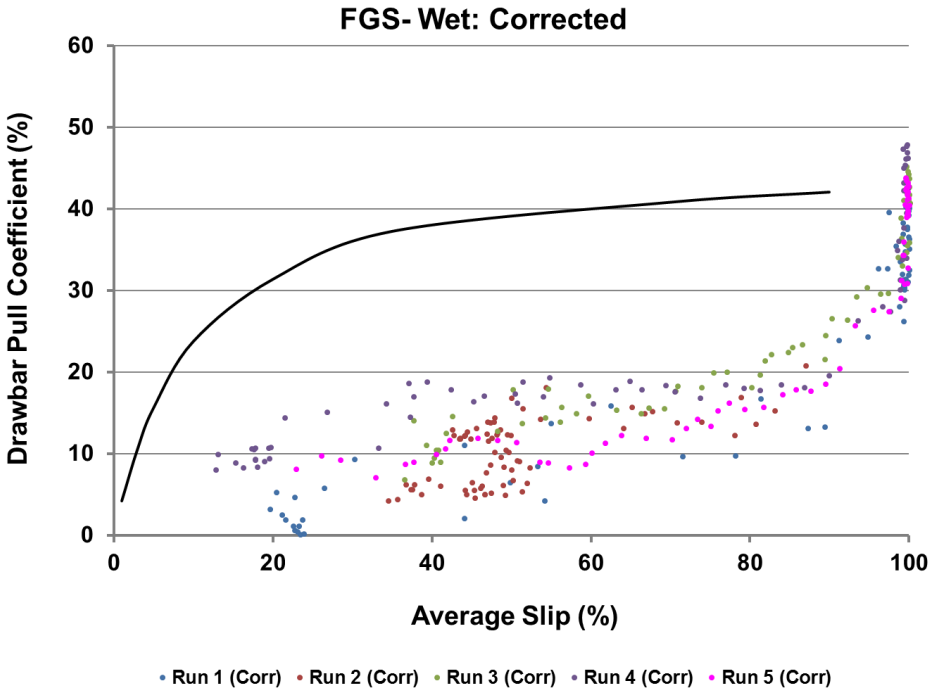

Figure Y-6: Comparison of the drawbar pull coefficient-slip relationship predicted by NWVPM (solid line) with that measured (with corrections for the inertial effect of vehicle mass) on fine-grained soil-wet of June 5, 2018.

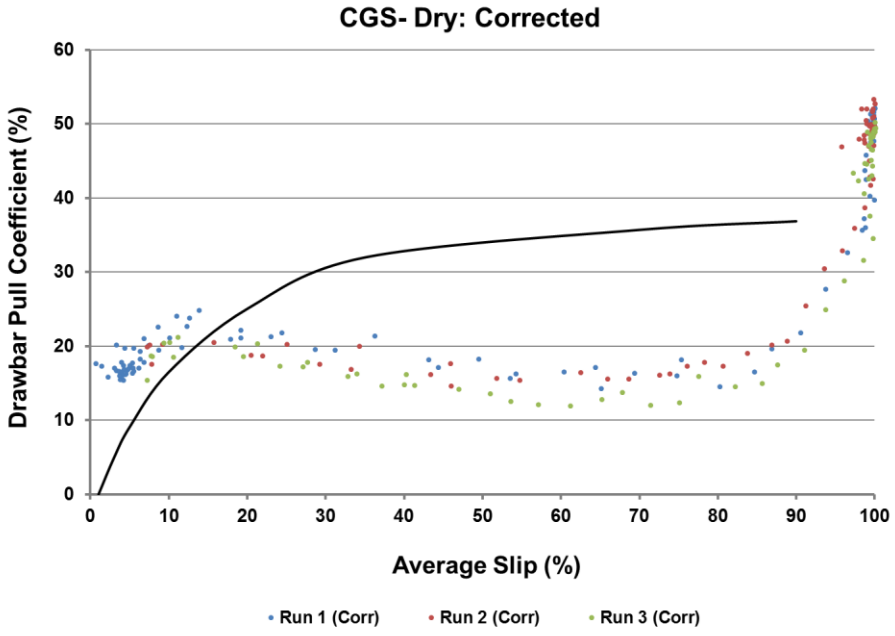

Figure Y-7: Comparison of the drawbar pull coefficient-slip relationship predicted by NWVPM (solid line) and that measured (with corrections for the inertial effect of vehicle mass on coarse-grained soil-dry of June 5, 2018.

Y.5.1.2 Vehicle drawbar performance predicted by NWVPM, based on terrain data obtained on June 5, 2018

The drawbar performance predicted by NWVPM on FGS-Dry, FGS-Wet, and CGS-Dry, based on terrain data obtained on June 5, 2018 and presented in Tables Y-3 and Y-4, are shown by solid lines in Figures Y-5, Y-6, and Y-7, respectively. It should be noted that the predicted performance are obtained with all wheels driven at the same slip, which is the necessary condition for achieving the optimal cross-country performance, as discussed in References [5, 6, 7, 8].

It should be mentioned that as shown in Figure Y-2, FGS - Dry is a very firm terrain. As a result, with the high values of repetitive loading parameters shown in Table Y-3, numerical difficulty was encountered in running the simulation model NWVPM, because of the high rigidity of the terrain. To overcome the numerical difficulty, the values of repetitive loading parameters k_0 and A_u were adjusted. Investigations were carried out to determine the effects of adjustments of the repetitive loading parameters on the predicted drawbar pull coefficient. Results of the investigations indicate that the adjustments of k_0 and A_u made would not have material effect on the predicted drawbar performance of the vehicle. As a result, the predicted drawbar pull coefficient-slip relationship on FGS - Dry shown in Figure Y-5 is considered acceptable.

It should be pointed out that in predicting the drawbar pull coefficient-slip relationships on FGS-Wet and CGS-Dry, shown in Figure Y-6 and Y-7, respectively, the values of repetitive loading parameters shown in Table Y-3 were used and no adjustments of their values were made. This is because these two types of terrain were softer than the FGS-Dry and no numerical difficulty was encountered.

The terrain data for 2NS Sand shown in Tables Y-3 and Y-4 were used to predict the gradeability of the FED-Alpha vehicle by NWVPM. On level 2NS Sand, the predicted drawbar pull coefficient at 20% slip is 28.29%. Consequently, if the motion resistance coefficient on a slope is assumed to be similar to that on level terrain, the maximum slope that the vehicle can climb at 20% slip under steady-state conditions, as limited by vehicle-terrain interaction, is 28.29% or 15.8º. At 90% slip, the predicted drawbar pull coefficient is 37.85%. Similarly the maximum slope that the vehicle can climb at that slip, as limited by vehicle-terrain interaction, is 37.85% or 20.8º.

The drawbar performance parameters over the range of slip from 1% to 100%, including the motion resistance coefficient (the ratio of motion resistance to vehicle weight), thrust coefficient (the ratio of thrust to vehicle weight), drawbar pull coefficient, tractive efficiency (the ratio of the product of drawbar pull and vehicle speed to the total power delivered to all driven wheels), and rut depth, of the FED-Alpha vehicle predicted by NWVPM on FGS-Dry, FGS-Wet, CGS-Dry, and 2NS Sand, with terrain data shown in Tables Y-3 and Y-4, are documented in Reference [9].

A comparison of the measured and predicted rut depths by NWVPM on FGS-Dry, FGS-Wet, and CGS-Dry is given in Table Y-7.

Table Y-7: Comparison of the measured and predicted rut depths by NWVPM on FGS-Dry, FGS-Wet, and CGS-Dry.

Date	Terrain	Test	Measured rut depth by KRC, cm	Predicted by NWVPM	
				Rut depth cm	Motion resistance coefficient, %
June 5, 2018	FGS-Dry	Drawbar	3 to 4	3.8	4.87 to 4.97
June 5, 2018	FGS-Wet	Drawbar	14 to 15	14.8 to 15.9	10.01 to 13.65
June 5, 2018	CGS-Dry	Drawbar	9 to 10	5.4 to 6	9.5 to 11.3

From Table Y-7, it can be seen that on FGS-Dry and on FGS-Wet, the measured rut depths are very close to that predicted by NWVPM. On CGS-Dry, there is a difference in rut depth between the predicted by NWVPM and that measured.

Y.5.1.3 Comparison of the measured vehicle performance under dynamic conditions with that predicted by NWVPM

On FGS-Dry terrain, as shown in Figure Y-5 the correlation between the measured drawbar performance with corrections for the inertial effect of vehicle mass and that predicted by NWVPM is very encouraging. The predicted drawbar pull coefficient-slip curve is within the measured data over the slip range from 0 to 90%.

On FGS-Wet terrain, as shown in Figure Y-6 there is substantial difference between the measured and predicted data. An examination of a sample of the test data designated as DB 8 reveals that the motion resistance derived from the difference between vehicle thrust, calculated from the measured torques delivered to the tires divided by the tire effective rolling radius (r=0.453 m), and the measured drawbar pull is substantial. This indicates that the

vehicle motion resistance (or motion resistance coefficient) during tests is high as shown in Table Y-8 (A). For instance, at data point No. 1 shown in Table Y-8 (A), the motion resistance coefficient is 22.29%. This is 2.03 times that of 10.97% predicted by NWVPM, as shown in Table Y-8 (B). It should be pointed out that vehicle motion resistance is closely related to rut depth. As shown in Table Y-7, on FGS-Wet the measured rut depth is essentially the same as that predicted by NWVPM. This indicates that the high motion resistance derived from the measured torque input to the tires and the measured drawbar pull do not appear to be consistent with the measured rut depth.

Table Y-8: Comparison of a Sample of Measured and Predicted Performance Data by NWVPM on FGS-Wet (June 5, 2018).

(A) Measured Performance Data by KRC (DB 8)

Data Point No.	Front axle		Rear axle		*Total Thrust (F_f+F_r) N	Drawbar pull (DP) N	**Derived motion resistance (R) N	**Derived motion resistance coefficient (R/W), %	Slip %
	Torque Nm	*Thrust (F_f), N	Torque Nm	*Thrust (F_r), N					
1	2,263	5,879	2,946	6,503	12,382	401	11,981	22.29	22.57
8	1,989	4,390	2.943	6,498	10,889	1,109	9,780	18.19	21.45
12	1,947	4,298	3,468	7,656	11,954	2,578	9,376	17.44	22.58
16	2,526	5,776	3,644	8,045	13,821	1,161	12,660	23.55	43.93
21	2,988	6,595	3,806	8,403	14,998	7,450	7,548	14.04	54.83

(B) Comparison of Measured and Predicted Motion Resistance Data

Data Point No.	**Derived motion resistance coefficient from measurements %	Predicted motion resistance coefficient by NWVPM %	**Derived motion resistance coefficient from measurements / Predicted by NWVPM	Slip %
1	22.29	10.97	2.03	22.57
8	18.19	11.02	1.65	21.45
12	17.44	10.97	1.59	22.58
16	23.55	10.45	2.25	43.93
21	14.04	10.32	1.36	54.83

Note:

*Measured axle thrust is assumed equal to the measured axle torque/tire effective rolling radius; tire effective rolling radius r = 0.453 m;

**Derived motion resistance is the difference between the sum of the measured axle thrusts noted above and the measured drawbar pull; derived motion resistance coefficient is the derived motion resistance normalized with respect to vehicle weight W = 53,755 N.

It should be pointed out that the measured axle thrust derived from the measured axle torque divided by the tire effective rolling radius is an approximation only. This is because the resultant shear force vector on the tire-terrain interface (with magnitude equal to the measured axle torque/tire effective rolling radius) may not be in the horizontal direction. Its direction, however, cannot be ascertained without elaborate instrumentation, which was not installed on the test vehicle. It should be noted that the direction of the resultant shear force vector is related to tire sinkage (rut depth). With the measured rut depth shown in Table Y-7, it is estimated that even if the angle between the resultant shear force vector and the horizontal is as high as 10º, the error in determining axle thrust by the measured axle torque divided by tire effective rolling radius would only be 1.5% (i.e., 1- cos10º). In view this, the value of the measured axle thrust, referred to in this study, is represented by the measured axle torque divided by tire effective rolling radius.

On CGS-Dry terrain, as shown in Figure Y-7 there is a reasonable correlation between the measured and predicted drawbar pull coefficient-slip relationships in the range of slip from 0 to 20%. Beyond that there is a substantial difference between the measured and predicted drawbar pull coefficient-slip relationships.

The substantial difference between the measured and predicted drawbar pull coefficient-slip relationships on FGS-Wet and that on CGS-Dry in the slip range beyond 20% may be due to a number of factors, some of which are outlined below:

(A) As noted previously, the original drawbar pull coefficient-slip relationship was measured under dynamic conditions, where the drawbar pull fluctuated widely and vehicle speed first increased up to a peak value and then decreased with time, which indicates the vehicle first accelerated and then decelerated, as shown in Figure Y-4 While the values of the measured drawbar pull coefficient have been corrected for the inertial effect of vehicle mass, as shown in Figures Y-5, Y-6, and Y-7, it is by no means certain that all other possible dynamic effects on vehicle-terrain interaction have been properly account for in the corrected drawbar pull coefficient-slip relationships. These would include the effects on performance of varying shear rate on the tire-terrain interface caused by the acceleration/deceleration of the vehicle, and of the fluctuation of the dynamic normal load on the tires caused by the variation of drawbar pull.

(B) The predictions of vehicle drawbar performance by NWVPM were based on the mean values of terrain parameters measured by KRC on only two locations on the FGS-Wet test site and on three locations on the CGS-Dry test site. In addition, it appears that there was a lack of measures to ensure the consistency of soil conditions on the test sites. Consequently, it is uncertain that the terrain data measured at only two or three spots would properly represent the overall terrain properties of the test sites where vehicle performance was measured. This would be a factor that contributes to the difference between the measured performance and that predicted by NWVPM.

(C) Previous studies on the performance of all-wheel-drive vehicles indicate that the necessary condition for achieving the optimal drawbar performance is the slips of all

driven wheels being equal [5, 6, 7, 8]. The drawbar performance of the FED-Alpha vehicle was predicted by NWVPM under the optimal condition, that is, the slips for all driven wheels are the same. An examination of the test data provided by KRC, such as the test set DB 8, reveals that the angular speeds of all driven wheels during tests were not the same in many cases, with a difference as high as 10.8%. This was inconsistent with the characteristics of the drivetrain of the FED-Alpha vehicle, which indicate that with the differentials of the front and rear axles locked, all driven wheels should be rotating at the same angular speed. This would seem to indicate that the accuracy of the measured data is uncertain or that the test data may contain considerable "noise". Furthermore, the vehicle performance parameters monitored during tests were not sufficient to enable the determination of the slip of individual driven wheels. Consequently, it cannot be ascertained whether the optimal drawbar performance of the vehicle was achieved during tests. This is another factor that would contribute to the discrepancy between the measured performance and that predicted by NWVPM.

(D) In summary, the causes for the discrepancies between the measured and predicted vehicle performance by NWVPM require in-depth investigation. This would involve a detailed review of the test procedures, equipment and instrumentation, test data, consistency of soil conditions on test sites, etc. Such a detailed examination is, however, beyond the scope of the tasks specified in the subcontract for VSDC.

Y.5.2 Comparison of the measured vehicle performance under steady-state conditions of June 29, 2018 with that predicted by NWVPM

As noted previously, steady-state drawbar performance is a cornerstone for evaluating off-road vehicle mobility, and the common practice is to conduct drawbar performance testing under steady-state conditions. As described in Section Y.5.1.1, the drawbar performance testing conducted on June 5, 2018 was under dynamic conditions. While corrections were made to the performance test data obtained under dynamic conditions to account for the inertial effect of vehicle mass, it is uncertain whether all other dynamic effects on vehicle-terrain interactions have been properly taken into account. To address this issue, additional set of vehicle performance testing under steady-state (or close to steady-state) conditions was performed on June 29, 2018. The drawbar pull coefficient-slip relationships thus obtained, with corrections for the minor inertial effect of vehicle mass, were compared with the predicted by NWVPM, based on the corresponding terrain data on the three types of terrain: FGS-Dry, FGS-Wet, and CGS-Dry, collected on June 29, 2018 and presented in Tables Y-5 and Y-6.

Y.5.2.1 Measured vehicle drawbar performance under steady-state conditions of June 29, 2018

The drawbar pull coefficient-slip curves measured under steady-state (or close to steady-state conditions with corrections for minor inertial effect of vehicle mass) on the three types of terrain, FGS-Dry, FGS-Wet, and CGS-Dry, are shown in Figures Y-8, Y-9, and Y-10, respectively.

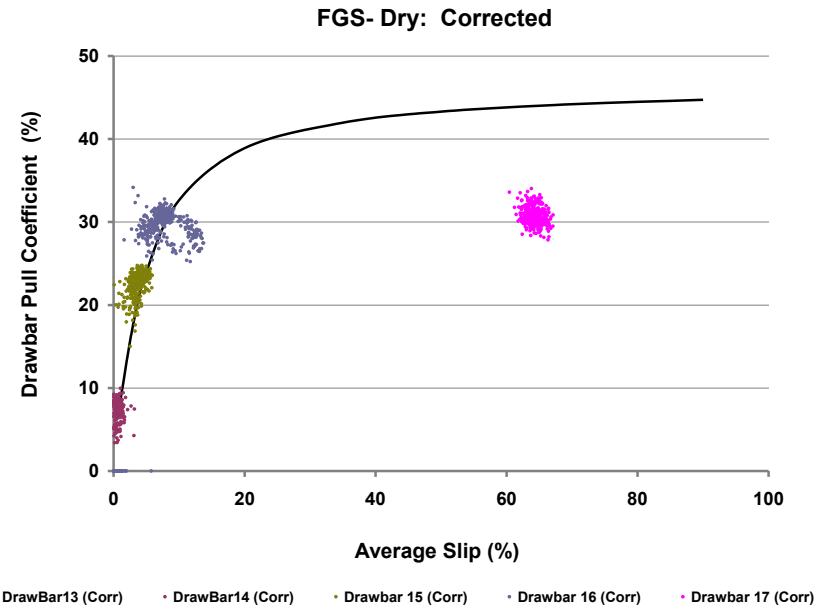

Figure Y-8: Comparison of the drawbar pull coefficient-slip relationship predicted by NWVPM (solid line) with that measured (with minor corrections to the inertial effect of vehicle mass) on fine-grained soil-dry of June 29, 2018.

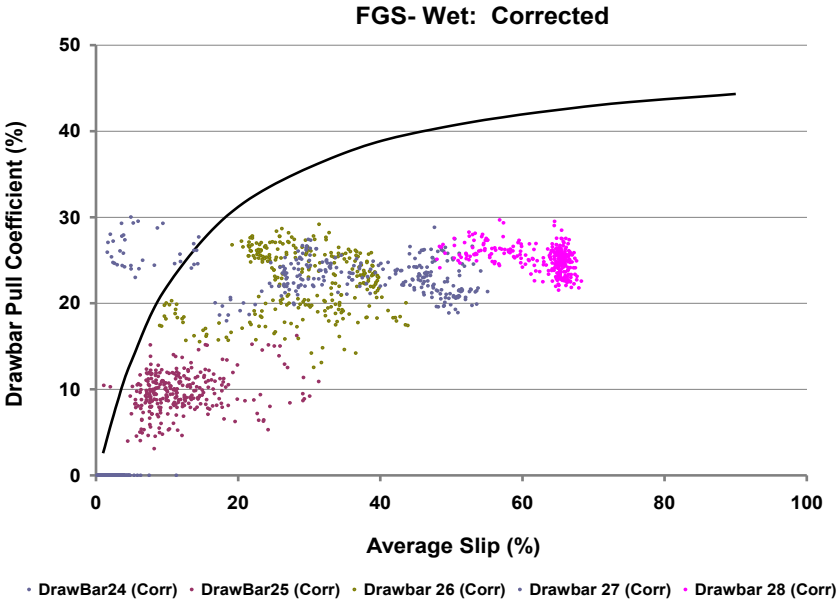

Figure Y-9: Comparison of the drawbar pull coefficient-slip relationship predicted by NWVPM (solid line) with that measured (with minor corrections to the inertial effect of vehicle mass) on fine-grained soil-wet of June 29, 2018.

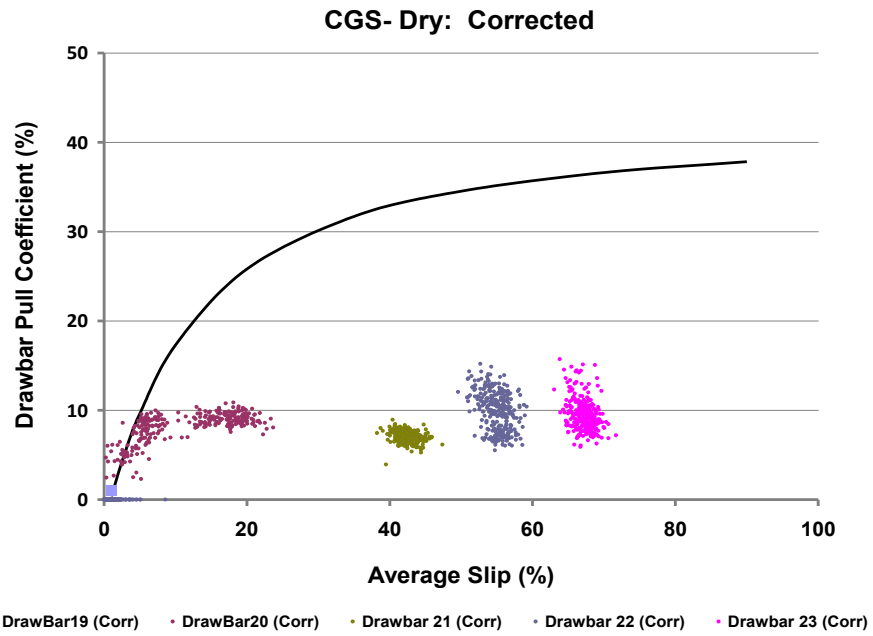

Figure Y-10: Comparison of the drawbar pull coefficient-slip relationship predicted by NWVPM (solid line) with that measured (with minor corrections to the inertial effect of vehicle mass) on coarse-grained soil-dry of June 29, 2018.

Y.5.2.2 Vehicle drawbar performance predicted by NWVPM, based on terrain data of June 29, 2018

The predicted drawbar performance obtained by NWVPM on FGS-Dry, FGS-Wet, and CGS-Dry, based on terrain data of June 29, 2018 presented in Tables Y-5 and Y-6, are shown by solid lines in Figures Y-8, Y-9, and Y-10, respectively.

Similar to that described in Section Y.5.1.2, as FGS-Dry is a very firm terrain, with the repetitive loading parameters shown in Table Y-5, numerical difficulty was encountered in running the simulation model NWVPM. To overcome the numerical difficulty, appropriate adjustments to the values of repetitive loading parameters k_0 and A_u were made. Similar to that mentioned in Section Y.5.1.2, investigations were carried out to determine the effects of adjustments of the repetitive loading parameters on the predicted drawbar pull coefficient. Results of the investigations indicate that the adjustments of k_0 and A_u would not have material effect on the predicted drawbar performance of the vehicle. As a result, the predicted drawbar pull coefficient-slip relationship on FGS-Dry represented by the solid line in Figure Y-8 is considered acceptable.

It should be pointed out that in predicting the drawbar pull coefficient-slip relationships on FGS-Wet and CGS-Dry, shown in Figure Y-9 and Y-10, respectively, the values of repetitive loading parameters shown in Table Y-5 were used and no adjustments in their values were made. This is because these two types of terrain were softer than the FGS-Dry and no numerical difficulty was encountered.

The drawbar performance parameters, including the motion resistance coefficient, thrust coefficient, drawbar pull coefficient, tractive efficiency, and rut depth, of the FED-Alpha vehicle predicted by NWVPM on FGS-Dry, FGS-Wet, and CGS-Dry, with terrain data presented in Tables Y-5 and Y-6, are documented in Reference [9].

Y.5.2.3 Comparison of the measured vehicle performance under steady-state conditions with that predicted by NWVPM

On FGS-Dry terrain, as shown in Figure Y-8 the correlation between the measured drawbar performance and that predicted by NWVPM is encouraging, particularly in low slip range. Beyond that the predicted drawbar pull coefficient-slip curve is, in general, not far from the measured data.

On FGS-Wet terrain, as shown in Figure Y-9 the correlation between the measured drawbar performance and that predicted by NWVPM is reasonable for the range of slip from 0 to 30%, approximately. Beyond that there is difference between the measured and predicted data.

In evaluating the correlation between the measured and predicted compressive stress distributions in the soil under a tire, Sohne suggested that "initial agreement between the measured and calculated values deviated by about 25 per cent, but nevertheless that allow an estimate to be made with reasonable accuracy" [10]. This would imply that in terramechanics, discrepancies between the measured and predicted data of the order of 25% may be considered as not unacceptable. If this view is adopted, then the correlations between the measured and predicted drawbar pull coefficient-slip relationship by NWVPM on FGS-Dry and FGS-Wet would be considered as not unreasonable.

On CGS-Dry, as shown in Figure Y-10 there is substantial difference between the measured drawbar pull coefficient vs. slip data obtained on June 29, 2018 by KRC and that predicted by NWVPM using terrain data obtained on the same date and presented in Tables Y-5 and Y-6. An examination of a sample of the test data designated as DB 21 provided by KRC reveals that the motion resistance derived from the difference between vehicle thrust, calculated from the measured torques delivered to the tires divided by tire effective rolling radius (r=0.453 m), and the measured drawbar pull is substantial. This indicates that the vehicle motion resistance (or motion resistance coefficient) during tests is high as shown in Table Y-9 A. For instance, at data point No. 1 shown in Table Y-9 (A), the motion resistance coefficient is 43.6%. In Table Y-9 (B), the values of the front axle thrust, rear axle thrust, the total vehicle thrust, drawbar pull, motion resistance, and motion resistance coefficient predicted by NWVPM are shown. Comparisons of the values of the thrust coefficient and that of the motion resistance coefficient derived from measured data with that predicted by NWVPM are presented in Table Y-9 (C).

It should be pointed out that from Table Y-9 (C) the values of the predicted thrust coefficient by NWVPM are close to that derived from measurements, and that over the range of slip shown in the table the difference varies in a narrow range of 6% to 11%. Figure Y-11 shows a comparison of the measured and predicted thrust coefficient (represented by the solid line)

over the slip range from 0 to 90%. It indicates that the correlation between the measured thrust coefficient-slip relationship and that predicted by NWVPM is reasonable, particularly for the range of slip below approximately 50%. **This provides evidence to substantiate that using the Bekker-Wong terrain parameters for CGS-Dry shown in Tables Y-5 and Y-6, vehicle thrust (or thrust coefficient) can reasonably be predicted by NWVPM.**

Table Y-9: Comparison of a Sample of Measured Performance Data under Steady-State Conditions and that Predicted by NWVPM on CGS-Dry (June 29, 2018).

(A) Measured Performance Data by KRC (DB 21)

Data point No.	Front axle		Rear axle		*Total Thrust (F_f+F_r) N	Drawbar pull (DP) N	**Derived motion resistance (R) N	**Derived motion resistance coefficient (R/W), %	Slip %
	Torque Nm	*Thrust (F_f), N	Torque Nm	*Thrust (F_r), N					
1	5,102	11,263	6,469	14,280	25,543	2,106	23,437	43.60	39.47
8	4,896	10,809	6,456	14,252	25,061	3,691	21,370	39.75	42.89
12	4,771	10,533	6,395	14,117	24,650	3,689	20,961	38.99	42.12
16	4,878	10,768	6,336	13,987	24,755	3,645	21,110	39.27	42.95
21	4,906	10,829	6,356	14,030	24,859	3,664	21,195	39.43	42.21

(B) Predicted Performance Data by NWVPM

Data point No.	Front axle thrust (F_f) N	Rear axle thrust (F_r) N	Total thrust (F_f+F_r) N	Drawbar pull (DP) N	Motion resistance (R) N	Motion resistance coefficient (R/W), %	Slip %
1	8,855	14,117	22,972	17,322	5,640	10.49	39.47
8	8,931	14,404	23,335	17,736	5,600	10.42	42.89
12	8,916	14,341	23,257	17,648	5,609	10.43	42.12
16	8,933	14,408	23,342	17,742	5,600	10.42	42.95
21	8,919	14,347	23,267	17,658	5,609	10.43	42.21

(C) Comparison of Measured and Predicted Performance Data

Data point No.	Thrust coefficient (F_f+F_r)/W			Motion Resistance coefficient (R/W)			Slip %
	**Derived from Measurements %	Predicted by NWVPM %	**Derived from Measurements/ Predicted by NWVPM	**Derived from measurements %	Predicted by NWVPM %	**Derived from measurements/ Predicted by NWVPM	
1	47.52	42.73	1.11	43.60	10.49	4.16	39.47
8	46.62	43.41	1.07	39.75	10.42	3.81	42.89
12	45.86	43.27	1.06	38.99	10.43	3.74	42.12
16	46.05	43.42	1.06	39.27	10.42	3.77	42.95
21	46.25	43.28	1.07	39.43	10.43	3.78	42.21

Note:

*Measured axle thrust is assumed equal to the measured axle torque/tire effective rolling radius; tire effective rolling radius r = 0.453 m;

**Derived motion resistance is the difference between the sum of the measured axle thrusts noted above and the measured drawbar pull; derived motion resistance coefficient is the derived motion resistance normalized with respect to vehicle weight W = 53,755 N.

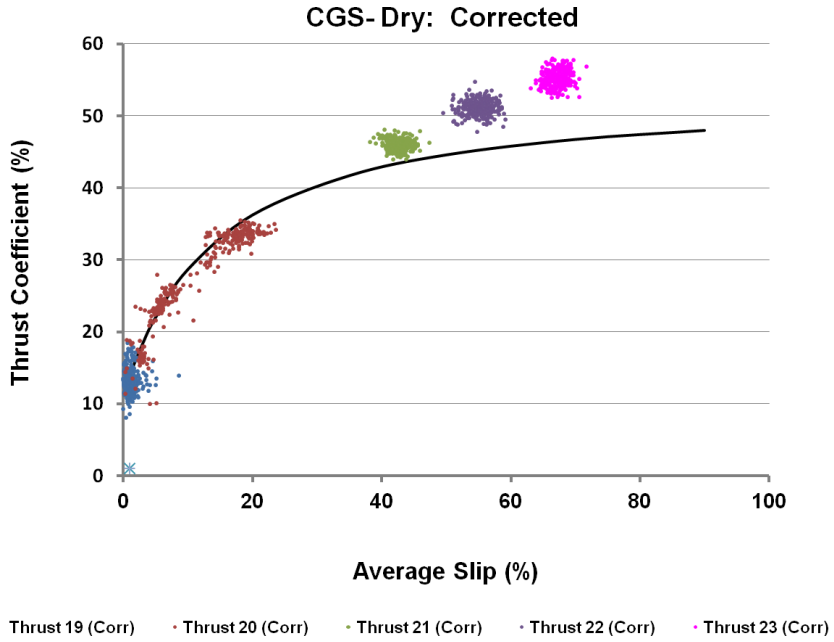

Figure Y-11: Comparison of the thrust coefficient-slip relationship predicted by NWVPM and that measured on coarse-grained soil-dry.

It should be pointed out, however, that there is a significant difference between the values of the derived motion resistance coefficient from measured data and that predicted by NWVPM, as shown in Table Y-9 (C). For the sample data shown, the ratio of the values of the derived motion resistance coefficient from measured data to that predicted by NWVPM varies from 3.74 to 4.16. The values of this ratio appear to be abnormally high. According to the analysis of the measured vehicle performance data of June 29, 2018 by McCullough [11], the mean values of the measured motion resistance coefficient and rut depth at zero drawbar pull on CGS-Dry, FGS-Dry and FGS-Wet are shown in Table Y-10. In the table, the values of the motion resistance coefficient and rut depth at zero drawbar pull predicted by NWVPM are also shown.

Table Y-10: Comparison of the mean values of the motion resistance coefficient and rut depth at zero drawbar pull derived from measured data with that predicted by NWVPM.

Date	Terrain	Data set	Mean value of motion resistance coefficient		Mean value of rut depth m	
			*Measured	Predicted by NWVPM	*Measured	Predicted by NWVPM
2018.06.29	CGS-Dry	DB 19	0.133	0.138	0.10	0.098
2018.06.29	FGS-Dry	DB 13	0.046	0.053	0.04	0.038
2018.06.29	FGS-Wet	DB 24	0.109	0.139	0.15	0.204

***Note*: *McCullough [11].**

From Table Y-10, the following observations may be made:

(A) On CGS-Dry, the value of the motion resistance coefficient of 0.138 at zero drawbar pull predicted by NWVPM is very close to the measured mean value of 0.133. The rut depth of 0.098 m at zero drawbar pull predicted by NWVPM is essentially the same as the measured mean value of 0.10 m.

(B) On FGS-Dry, the value of the motion resistance coefficient of 0.053 at zero drawbar pull predicted by NWVPM is reasonably close to the measured mean value of 0.046. The rut depth of 0.038 m at zero drawbar pull predicted by NWVPM is very close to the measured mean value of 0.04 m.

(C) On FGS-Wet, the value of the motion resistance coefficient of 0.139 at zero drawbar pull predicted by NWVPM is reasonably close to the measured mean value of 0.109. The rut depth of 0.204 m at zero drawbar pull predicted by NWVPM is not significantly different from the measured mean value of 0.15 m.

All these indicate that in general, at zero drawbar pull the correlations between the values of the motion resistance coefficient and rut depth predicted by NWVPM and that measured are reasonably close on the three types of terrain examined. **This provides evidence to substantiate the capability of NWVPM to predict the motion resistance coefficient and rut depth of the FED-Alpha vehicle using the Bekker-Wong terrain parameters. Furthermore, as noted previously, NWVPM provides reasonable predictions of thrust coefficient on CGS-Dry and the drawbar pull coefficient is the difference between the thrust coefficient and motion resistance coefficient, this implies that the drawbar pull coefficient-slip relationship on CGS-Dry predicted by NWVPM would be reasonable.**

It should be pointed out that while vehicle motion resistance at zero drawbar pull may not be the same as that at non-zero drawbar pull, the derived motion resistance (or motion resistance coefficient) from measured data for the slip range of 39.47% to 42.95% being approximately 4 times that predicted by NWVPM on CGS-Dry, as shown in Table Y-9 (C), is abnormal. The discrepancy between the measured drawbar pull (or the derived motion resistance from measured data) and that predicted by NWVPM may be caused by a number of factors, similar to those discussed in Section Y.5.1.3. For instance, the values of the terrain parameters, upon which vehicle drawbar performance was predicted by NWVPM, were obtained with only one set of tests on one location. It is uncertain that the overall terrain properties on the test site can be properly represented by only one set of test data taken at one location. In addition, the validity of some of the performance test data is uncertain. For instance, an examination of some of the test data provided by KRC, such as the test set DB 21, reveals that the angular speeds of all driven wheels in many cases during tests were not the same, with a difference as high as 12.2%. This was inconsistent with the characteristics of the drivetrain of the FED-Alpha vehicle provided by the vehicle manufacturer, which indicated that with the differentials of the front and rear axles locked, all driven wheels should be rotating at the same angular speed. This would indicate that the validity of some of the measured data is uncertain or that the test data may contain considerable “noise”. Furthermore, as indicated previously, NWVPM predicts the optimal drawbar performance for which all driven wheels slip at the same rate. However, it is uncertain whether the measured vehicle performance was at its

optimal during tests. This is because some of the vehicle performance test data required, such as the slip of all individual tires, was not monitored during tests.

To investigate the anomalies in the measured performance data, such as the drawbar pull coefficient-slip relationship on CGS-Dry, a detailed review is required of the test procedures, equipment and instrumentation, test data, consistency of soil conditions on the test sites, etc. Such a detailed examination is, however, beyond the scope of the tasks specified in the subcontract for VSDC.

Y.6 SIMULATIONS OF VEHICLE PERFORMANCE AT DESIGN OF EXPERIMENT (DOE) POINTS BY NWVPM FOR UNCERTAINTY QUANTIFICATION MAPS

The tractive capability of the FED-Alpha vehicle may be represented by its drawbar pull coefficient at 90%. This was predicted by NWVPM at design of experiment (DOE) points for uncertainty quantification maps. These include predictions of vehicle performance at 90 DOE points for sand, sandy loam and silt, at 18 DOE points for pavement, gravel and crushed rock, and at 50 DOE points for peat, specified by RAMDO Solutions. The values of the major terrain parameters at DOE points were provided by RAMDO Solutions. The values of some of the terrain parameters not provided by RAMDO Solutions were assumed by VSDC, based on the values for similar terrains in its data bank.

The drawbar pull coefficient at 90% slip on a slope is estimated by [12]
$(D/W)_{slope} = (D/W)_{level} - Slope\ (\%)$
where $(D/W)_{slope}$ is the drawbar pull coefficient at 90% slip on a slope; $(D/W)_{level}$ is the drawbar pull coefficient at 90% slip on level terrain. If the value of $(D/W)_{slope}$ is negative, it will indicate that the vehicle is NoGo on that slope, or the vehicle is not capable of operating under steady-state conditions on that slope.

The results of vehicle performance predictions by NWVPM at DOE points on various types of terrain submitted to RAMDO Solutions are documented in Reference [9].

It should be noted that the provision of simulation results obtained using VSDC's software NWVPM for the uncertainty quantification maps (UQM) does not necessarily constitute or imply its endorsement, recommendation, or favoring by VSDC of the methodology used for producing UQM, and does not necessarily constitute or imply any warranty, expressed or implied, by VSDC on the validity or accuracy of the UQM based on the simulation results provided by VSDC.

Y.7 CLOSING REMARKS

(A) This report summarizes the results of using the Nepean Wheeled Vehicle Performance Model (NWVPM), developed by Vehicle Systems Development Corporation, Toronto, Ontario, Canada, to predict the drawbar performance of the FED-Alpha vehicle on various types of terrain and to compare them with test data obtained by Keweenaw Research Center, Michigan Technological University.

(B) Steady-state drawbar performance is a cornerstone for evaluating off-road vehicle mobility. Consequently, it is a common practice in both military and civilian sectors to conduct drawbar performance testing under steady-state conditions.

(C) If vehicle drawbar performance testing is conducted under dynamic (time-varying or transient) conditions, then even if the results are corrected for the inertial effect of vehicle mass, it will still be uncertain that this correction alone could account for all other possible dynamic effects on vehicle-terrain interaction, such as the effect on performance of varying shear rate at the tire-terrain interface caused by the variation of vehicle speed, and of the fluctuation of dynamic normal load on the tires caused by the variation of drawbar pull.

(D) To provide valid vehicle performance test data for evaluating the predictions by simulation models on deformable terrain, consistency of terrain conditions on test sites is of importance and should be carefully monitored. For vehicle performance tests conducted on June 29, 2018, for instance, only one set of terrain data was taken on each test site. It is uncertain that one set of terrain data obtained at one location could adequately represent terrain properties of the entire test site. Consequently, this could have a significant impact on the correlation between the predicted and measured data.

(E) The results show that on the FGS-Dry, the correlation is very encouraging between the measured drawbar performance, obtained under dynamic conditions but corrected for the inertial effect of vehicle mass, and that predicted by NWVPM. The predicted drawbar pull coefficient-slip curve is within the measured data over an extended slip range.

(F) On FGS-Wet, there is a substantial difference between the measured drawbar pull coefficient-slip relationship, obtained under dynamic conditions but corrected for the inertial effect of vehicle mass, and that predicted by NWVPM. The major reason is the significant discrepancy between the derived motion resistance, from the measured axle torques and measured drawbar pull, and that predicted by NWVPM. It is shown, however, that the measured rut depth is very close to that predicted by NWVPM on FGS-Wet. It is generally accepted that the motion resistance is closely related to rut depth. This indicates that the anomalies in the derived motion resistance from measured axle torques and measured drawbar pull require detailed investigation.

(G) On CGS-Dry, there is a reasonable correlation between the measured drawbar pull coefficient, obtained under dynamic conditions but corrected for the inertial effect of vehicle mass, and that predicted by NWVPM in the slip range from 0 to 20%. Beyond that there is a substantial difference between the measured and predicted drawbar pull coefficient-slip relationship. The anomalies require an in-depth examination.

(H) The correlations between the drawbar pull coefficient-slip relationships measured under steady-state (or close to steady-state) conditions and that predicted by NWVPM on FGS-Dry and FGS-Wet appear to be not unreasonable, if the view that in terramechanics, a discrepancy between the measured and predicted data is around 25% is considered acceptable.

(I) On CGS-Dry, there is a substantial difference between the drawbar pull coefficient-slip relationship measured under steady-state (or close to steady-state) conditions and that predicted by NWVPM. It should be pointed out, however, that

(a) the values of the thrust coefficient predicted by NWVPM are close to that derived from the measured axle torques divided by tire effective rolling radius over the slip range from 0 to 90%. This indicates that the capability of

NWVPM to predict the thrust coefficient-slip relationship based on the Bekker-Wong terrain parameters is substantiated;

(b) the values of the motion resistance coefficient and rut depth at zero drawbar pull predicted by NWVPM are close to that measured [11]. This indicates that the approach of using the Bekker-Wong terrain parameters and NWVPM to predicting vehicle motion resistance and rut depth is substantiated;

(c) As the drawbar pull coefficient is the difference between the thrust coefficient and motion resistance coefficient, this implies the drawbar pull coefficient-slip relationship on CGS-Dry predicted by NWVPM would be reasonable.

(J) As noted in (I), it appears that the anomalies in the measured drawbar pull coefficient-slip relationship on CGS-Dry require an in-depth investigation. Such an investigation would require a detailed review of the test procedures, test equipment and instrumentation, test data, consistency of soil conditions on test sites, etc. This type of in-depth review is, however, beyond the scope of the tasks stipulated in the subcontract for VSDC.

(K) To quantitatively examine the correlation between measured and predicted data, metrics such as the coefficient of correlation *R,* the coefficient of determination R^2, the root mean square deviation *RMSD,* the coefficient of variation *CV* and the like, should be used. This should be considered in the evaluation of the correlation between measured and predicted data in future studies.

Y.8 GAPS AND PATH FORWARD

In the development of the Standardization Recommendation for the Next-Generation NATO Reference Mobility Model (NG-NRMM), it is necessary to have an adequate database for verification and validation of modeling and simulation methods, and for establishing maturity scales and practical benchmarks. It is recommended that the following be implemented:

(A) In addition to the database for terrain topography and scenario, establishing an adequate database for engineering properties of terrain of interest to NATO military operations.

This would include the database of engineering properties of terrain for both the simple and complex terramechanics types. This database may be developed through remote sensing of physical properties of terrain, such as moisture content, density, void ratio and the like, and of terrain types based on the Unified Soil Classification System. This requires concerted efforts in research and development to establish comprehensive correlations between physical properties and engineering properties of terrain of interest to the NATO community, for both the simple and complex terramechanics types.

(B) Establishing a sufficient performance test database for representative vehicle types of interest to the NATO community.

(C) In evaluating modeling and simulation methods, using metrics, such as coefficient of correlation, coefficient of determination, root mean square deviation, coefficient of variation, and the like, to quantitatively examine the correlations between measured data and predictions.

Acknowledgements

The work described in this chapter was performed by Vehicle Systems Development Corporation, Toronto, Ontario, Canada, under Subcontract No. SFP1147916, administered by Alion Science and Technology Corporation, U.S.A., for the U.S. Army Tank Automotive Research, Development and Engineering Center, Warren, Michigan, U.S.A.

Disclaimer

Reference herein to any specific commercial company, product, process or service by trade name, trademark, manufacturer or otherwise does not necessarily constitute or imply its endorsement, recommendation or favouring by the U.S. Government or the Department of the Army (DoA). The opinions of the author expressed herein do not necessarily state or reflect those of the U.S. Government or the DoA and shall not be used for advertising or product endorsement purposes.

REFERENCES

1. Wong, J.Y. *Terramechanics and Off-Road Vehicle Engineering,* 2nd Edition. Oxford, England: Elsevier, 2010.

2. Wong, J.Y. *Theory of Ground Vehicles,* 4th Edition. New Jersey: John Wiley, 2008.
3. Bekker, M.G. *Introduction to Terrain-Vehicle Systems.* Ann Arbor, MI: The University of Michigan Press, 1969.

4. Janosi, Z. and Hanamoto, B. The analytical determination of drawbar pull as a function of slip for tracked vehicles in deformable soils. Proceedings of the First International Conference on the Mechanics of Soil-Vehicle Systems, Edizioni Minerva Tecnica, Torino, Italy, 1961.

5. Wong, J.Y. Optimization of the tractive performance of four-wheel-drive off-road vehicles. *SAE Transactions,* 79, 2238-2246, 1970.

6. Wong, J.Y., McLaughlin, N.B., Knezevic, Z., and Burtt, S. Optimization of the tractive performance of four-wheel-drive tractors: theoretical analysis and experimental substantiation. *Journal of Automobile Engineering,* Proceedings of the Institution of Mechanical Engineers, 212(D4), 285-297, 1998.

7. Wong, J.Y., Zhao, Zhiwen., Li, Jianqiao., McLaughlin, N.B., and Burtt, S. Optimization of the tractive performance of four-wheel-drive tractors - correlation between analytical predictions and experimental data. *SAE Transactions,* Section 2*, Journal of Commercial Vehicles,* Paper 2000-01-2596, 2000.

8. Huang, Wei., Wong, J.Y., and Knezevic, Z. Further study of the optimization of the tractive performance of all-wheel-drive vehicles. *International Journal of Heavy Vehicle Systems,* 21(2), 123-151, 2014.

9. Vehicle Systems Development Corporation. Milestone Report (Revised), CDT Phase II Study – Comparison of drawbar performance of the FED-Alpha vehicle predicted by NWVPM with test data on various types of terrain. Report for Alion Science and Technology Corporation, under Subcontract No. SFP1147619, November 2018.

10. Sohne, Walter. Agricultural engineering and terramechanics. Journal of Terramechanics, 6(4), pp. 9-30, 1969.

11. McCullough, Michael. Simple Terramechanics in the Next Generation-NATO Reference Mobility Model (NG-NRMM). AVT-308 Cooperative Demonstration of Technology on Next-Generation NATO Reference Mobility Model Development, Keweenaw Research Center, Michigan Technological University, Houghton, Michigan, U.S.A., September 25-27, 2018.

12. Baylot, E.A. et al. Standard for ground vehicle mobility. Report ERDC/GSL TR-05-6. U.S. Army Corps of Engineers, Engineer Research and Development Center, February 2005.